

# **WETTABILITY IMPACT ON CO<sub>2</sub> STORAGE IN AQUIFERS: VISUALISATION AND QUANTIFICATION USING MICROMODEL TESTS, PORE NETWORK MODEL AND RESERVOIR SIMULATIONS**

C. Chalbaud, M. Robin, S. Bekri and P. Egermann\* (\*Now with Gaz de France)  
Institut Français du Pétrole (IFP)

*This paper was prepared for presentation at the International Symposium of the Society of Core Analysts held in Calgary, Canada, 10-12 September, 2007*

## **ABSTRACT**

Wettability has been recognized as one of the controlling parameters of the remaining fluid saturations, capillary pressure and relative permeability curves; hence conditioning the performance of any CO<sub>2</sub> injection process either for storage or IOR purposes. This paper presents an integrated study based on experimental and theoretical methods (micromodel tests and pore-network model respectively) and numerical simulations to evaluate in a comprehensive and robust manner, the impact of different wettability scenarios, at the core scale for CO<sub>2</sub> injection in an aquifer. Some of the results observed in the micromodels were integrated in a pore network model in order to obtain capillary pressure and relative permeability curves, for various CO<sub>2</sub>/brine wettability conditions. Then, these curves and a compositional simulator dedicated to CO<sub>2</sub> injection processes were used to quantify the impact of these different wettability scenarios on injectivity at the core scale and at the near wellbore scale. Using this approach, it is possible to investigate at a larger scale the effects of the wetting phenomena that are observed at the pore scale. Although the work presented in this manuscript does not include the main geological features (heterogeneities), the results obtained so far clearly demonstrate the importance of using reliable wettability data at reservoir conditions for the accuracy of the prediction of CO<sub>2</sub> injection models at the reservoir scale.

## **INTRODUCTION**

In CO<sub>2</sub> geological storage projects, two critical issues must be addressed to make sure that this process is a feasible strategy to stabilize carbon dioxide concentration in the atmosphere: the location and distribution of the injected CO<sub>2</sub>, and the demonstration that it will remain stored in the long term; that has been defined by the IEA-GHG (2004) as a period ranking from several hundreds to several thousands years. The first issue refers to CO<sub>2</sub> behavior in the reservoir rock and the second to its eventual invasion of the caprock, a low permeable and usually shaly porous material saturated with water. On the one hand, there is a risk for upward migration enhanced by the CO<sub>2</sub> buoyancy because CO<sub>2</sub> in sedimentary basins is always lighter than formation water. On the other hand, possible leakage through existing wells needs to be considered (Nordbotten *et al.*, 2005) because this type of storage is likely to occur in mature basins using existing infrastructure. In order to have a better understanding of these issues and in order to develop quantitative tools to analyze these situations, wettability should be taken into account.

The idea was to start from the microscopic scale, physical properties and rock/fluid interactions (microscopic observation of fluid distribution and wetting fluid films on the pore walls in micromodels). The results were then introduced in a Pore Network Model to provide data from the modeling of experiments at the core scale, data which have been used afterwards for simulations at the reservoir scale.

Wettability is defined as the tendency of one fluid to spread on or adhere to a solid surface in the presence of other immiscible fluids (Craig, 1971). In the case of a CO<sub>2</sub> flooding operation, it determines the fluid distribution in the reservoir because it affects the quantity displaced as well as how the displacement proceeds. For aquifers, a brine-CO<sub>2</sub> system, if the rock is water-wet, there is a tendency for water to occupy the small pores and to contact most of the rock surface. Similarly, if the injected CO<sub>2</sub> eventually wets the surface, the carbon dioxide will occupy the small pores and will contact the majority of the rock surface. In both cases, the wetting fluid will occupy the small pores and will be present in the largest pores as a film on the rock surface. The existence of such a film enhances the continuity of the wetting phase, affecting the petrophysical properties of the reservoirs; among them the relative permeability and the capillary pressure curves, and therefore the injectivity level associated to a reservoir formation.

Concerning the leakage of the stored CO<sub>2</sub>, its invasion in the caprock may occur according to different physical mechanisms: capillary breakthrough of the CO<sub>2</sub> phase, diffusion of CO<sub>2</sub> molecules into brine and migration through reactivated or induced fractures in the caprock consecutively to a pressure build up or a temperature decrease during CO<sub>2</sub> injection.

This paper focuses on the effects of wettability on the mechanisms mentioned above. Capillary breakthrough occurs when the pressure of the CO<sub>2</sub> phase rises above a threshold value which corresponds to the capillary threshold pressure:

$$P_c^{th} = P_{CO_2} - P_{brine} = \frac{2\gamma \cos \theta}{R_{throat}^{max}} \quad (1)$$

where the  $P_c^{th}$  is the capillary pressure value that has to be exceeded before the non-wetting phase can start to drain the porous medium and flow,  $\gamma$  is the interfacial tension,  $\theta$  is the contact angle and  $R_{throat}^{max}$  corresponds to the largest connected pore throats or microfractures in the caprock. This displacement pressure is routinely measured in the evaluation of natural gas reservoir storage reservoirs (Thomas *et al.*, 1968). More information about this pressure value and how to measure it from laboratory tests can be founded elsewhere (Egermann *et al.*, 2006a).

In two-phase and three-phase systems, the gas, in most cases, is considered as the non-wetting fluid. This generalization usually leads to neglect the possibility of a partial wettability (and its consequences) of the injected CO<sub>2</sub>, even if, at storage conditions, it is not a gas phase but rather a supercritical phase or a liquid phase. Recently, Chiquet *et al.* (2004) measured the contact angle between brine, dense CO<sub>2</sub> and minerals representative of shale, such as mica and quartz. The authors reported that these minerals turn out from a strongly water-wet system at low pressures (gas CO<sub>2</sub>) to an intermediate wet system at higher pressures (dense CO<sub>2</sub>). According to the authors, such contact angle variations are

primarily the consequence of the reduction, at high pressures (low pH), of electrostatic interactions at the interfaces. These interactions tend to stabilize the brine film and favor water-wettability. A similar change from water-wet to intermediate wet conditions while increasing pressure was reported by Siemons et al. (2005) for coal-water-CO<sub>2</sub> systems by means of contact angle measurements. At the core scale, Egermann et al. (2006b) by means of standard CO<sub>2</sub> flooding experiments in carbonate cores at reservoir conditions observed that for pressures from 80 to 180 bar and temperatures from 60 to 80 °C, the CO<sub>2</sub> is clearly the non wetting phase. These results seem to disagree with those reported by Chiquet et al. (2004), since, in carbonate rocks, the isoelectric point or the point where the surface charge density vanishes occurs at a lower pressure. Therefore, if the wettability alteration while increasing pressure can be attributed to the electrostatic forces, this alteration should be more important for carbonate minerals, which is not the case according to Egermann et al. (2006b). This point needs further investigation since these experiments were conducted under different conditions which make hard to compare them directly.

Due to apparent contradictions of the results existing in the literature concerning the possibility of a partial CO<sub>2</sub> wettability on minerals, we carried out experimental injection tests, using glass micromodels at different pressures and temperature conditions and different wettability scenarios. In order to evaluate the consequences of these observations on CO<sub>2</sub> storage, we used a numerical percolation-type network model and numerical reservoir simulations. This allows upscaling from the pore scale to the core scale and from the core scale to the reservoir scale.

The paper is organized as follows. The first section describes the experimental set-up, the experimental conditions and the procedure which was used. In the second section, we present our results which are discussed and compared with those of previous works, some of them presented in the Introduction. The third section is dedicated to the application of these results to practical storage cases, especially in deep saline aquifers. Finally, conclusions are drawn on the future work to be conducted.

## **EXPERIMENTAL SECTION**

A pressurized micromodel was used to visualize the phase distribution and mobilization under a CO<sub>2</sub> flooding in water saturated porous media. Different thermodynamic conditions were investigated to cover the three physical states of CO<sub>2</sub>: gas, liquid and supercritical. Three wettability conditions were investigated: water-wet (WW), intermediate wet (IW) and oil wet (OW).

### **Experimental Set-up**

A two-dimensional heterogeneous pore structure is etched onto the surface of a completely flat glass plate. The size of the 2D pore network is 6.55 cm x 1.25 cm. The structure is only one pore depth. This depth is about 0.3 mm. Glass plates are naturally water-wet. In order to change the surface to strongly oil-wet, we have treated the surface with a silane. Another micromodel, naturally water-wet, was treated to intermediate-wet by ageing the surface with an asphaltic crude oil. In both cases, wettability conditions were verified by means of contact angle measurements on treated glass plates. The pore

distribution of the oil-wet and the intermediate-wet micromodel was the same. A schematic diagram of the experimental set-up is given in Fig. 1. The micromodel can be operated up to 100 bar and 60°C.

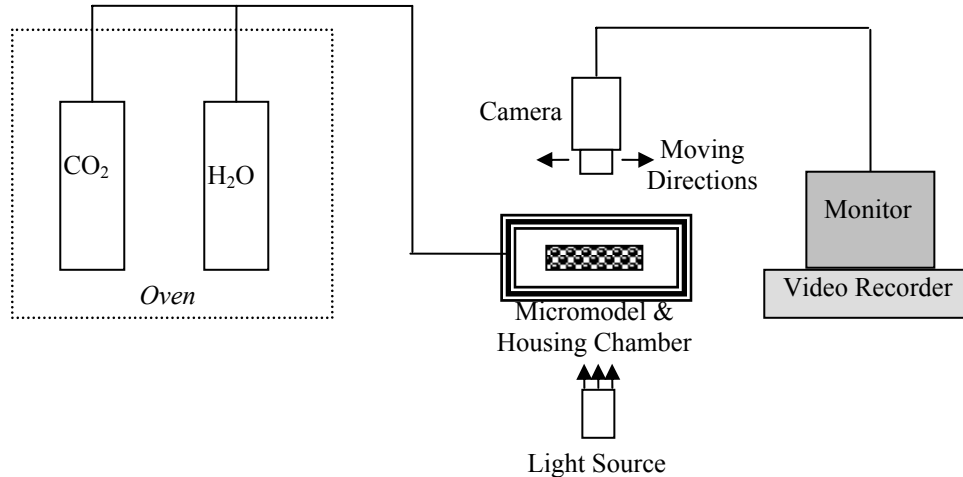


Figure 1. Experimental set-up for micromodel visualisation

### Experimental Procedure

The following procedure was followed in all the reported tests. Initially, the micromodel was saturated with distilled water at ambient conditions. Once the micromodel and the CO<sub>2</sub> were stabilized at the desired pressure and temperature, the CO<sub>2</sub> was injected at a low flow rate (1 cm<sup>3</sup>/h). The evolution of the phase distribution was recorded. After about 30 minutes the phase distribution remained constant. Changes observed during this time correspond to the evolution of the saturations of the pore network till a stabilized CO<sub>2</sub> saturation. It depends on the thermodynamic conditions, and on the dissolution of CO<sub>2</sub> into water. The results reported in this study correspond to the images after this stabilization. Once this static state was recorded along the micromodel, a flush of distilled water was injected in order to get the initial state and the desired pressure was adjusted.

### Experimental Results

Figures 2, 3 and 4 present the phase distribution after stabilization for CO<sub>2</sub> flooding in water saturated micromodels. For gaseous and supercritical CO<sub>2</sub>, we can identify the phases since the darkest phase is always the CO<sub>2</sub> phase. For liquid CO<sub>2</sub>, this is a little more difficult because its color is very close to the one corresponding to the water phase. For all the micromodel pictures, the average size of the circular grains (circles) is 0.3 mm.

#### Experiments with water-wet micromodels (Fig. 2, Fig. 3)

In water-wet micromodels and low pressures (gaseous CO<sub>2</sub>) we have observed very thin water films surrounding the solid surface (Fig. 2a and Fig. 3a). At higher pressures (Figures 3b and 3c), it is much more difficult to observe such films. Roughness could affect the observation of these films. However, it is important to note that the same micromodel has been used in these 3 experiments. The evolution of the film thickness is directly related to the relative affinity between water, CO<sub>2</sub> and the solid substrate. The

estimation of this affinity is not simple since it needs many physico-chemical parameters to be taken into account and most of them are not available in the literature. Chiquet et al.'s work (2004) presented in the Introduction could help to explain this thickness reduction. The authors attribute this behavior to a reduction in electrostatic interaction that tends to stabilize the water films. This explanation is based on the DLVO theory (Derjaguin and Landau, 1941 and Verwey and Overbeek, 1948). Despite this behavior, the shape of the interfaces (Figure 3) shows that there is no transition from a water-wet system to an intermediate-wet system while increasing pressures up to 100 bar. That is to say that if the solid was originally water-wet, it keeps strong water wettability at higher pressures, and water always remains a connected phase. This is coherent with the wettability indices deduced by Egermann et al. (2006b) from the injection of CO<sub>2</sub> performed in carbonate samples and presented in the Introduction.

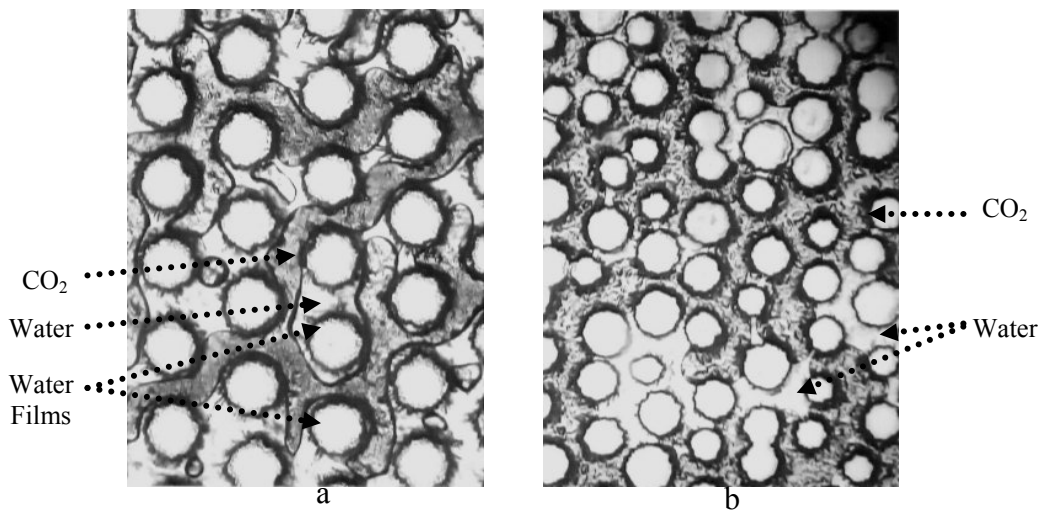


Figure 2: Gaseous CO<sub>2</sub> (5 bar, 20 °C): (a) water-wet micromodel - (b) intermediate-wet.

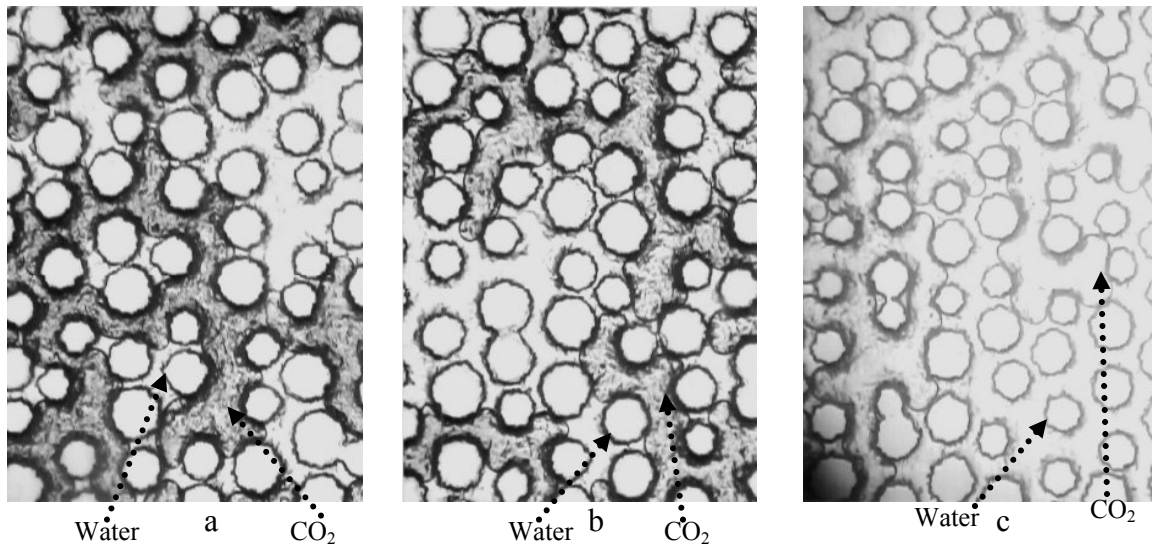


Figure 3: Water-wet micromodel: (a) gaseous CO<sub>2</sub> (57.9 bar, 20 °C) – (b) supercritical CO<sub>2</sub> (105.4 bar-60°C) – (c) liquid CO<sub>2</sub> (100 bar, 23 °C)

Experiments with oil-wet and intermediate-wet micromodels (Fig. 2, Fig. 4, Fig. 5)

In Fig. 2b, it is not possible to observe water films around the pores. This contrasts with the same thermodynamic conditions in a water-wet micromodel (Fig. 2a). The results obtained for these two wettability conditions are similar: at low pressures, the water is still the wetting phase. This corresponds to the current assumption considering the gas as the non-wetting phase, compared to a liquid. Nevertheless, it is important to mention that some interfaces (Fig. 4a and 5a) show that this water wettability was weaker for the intermediate-wet micromodel.

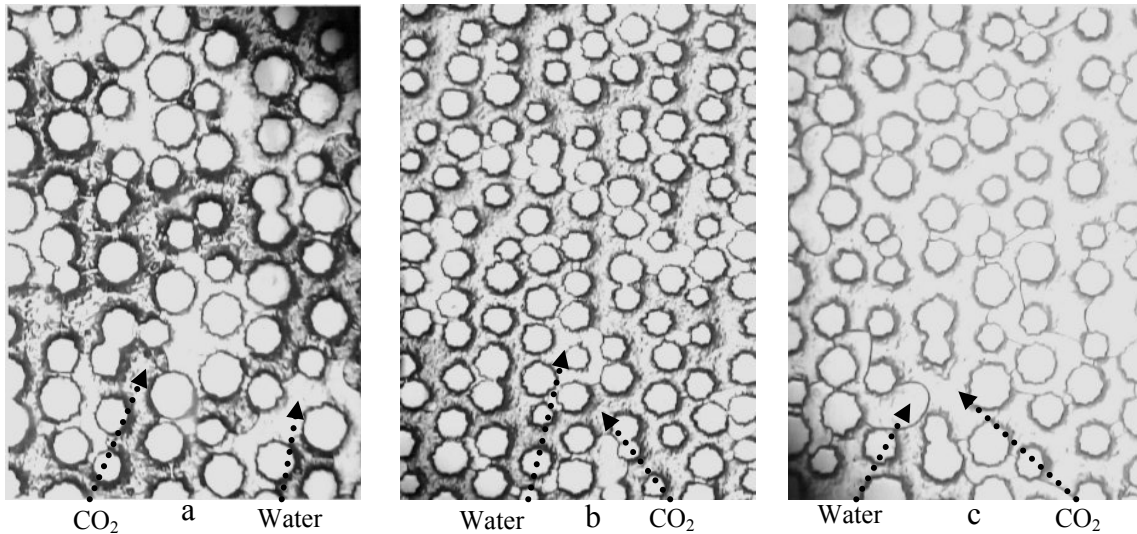


Figure 4: Oil-wet micromodel: (a) gaseous  $\text{CO}_2$  (51.3 bar,  $19^\circ\text{C}$ ) – (b) supercritical  $\text{CO}_2$  (100 bar,  $60^\circ\text{C}$ ) – (c) liquid  $\text{CO}_2$  (100bar,  $23^\circ\text{C}$ )

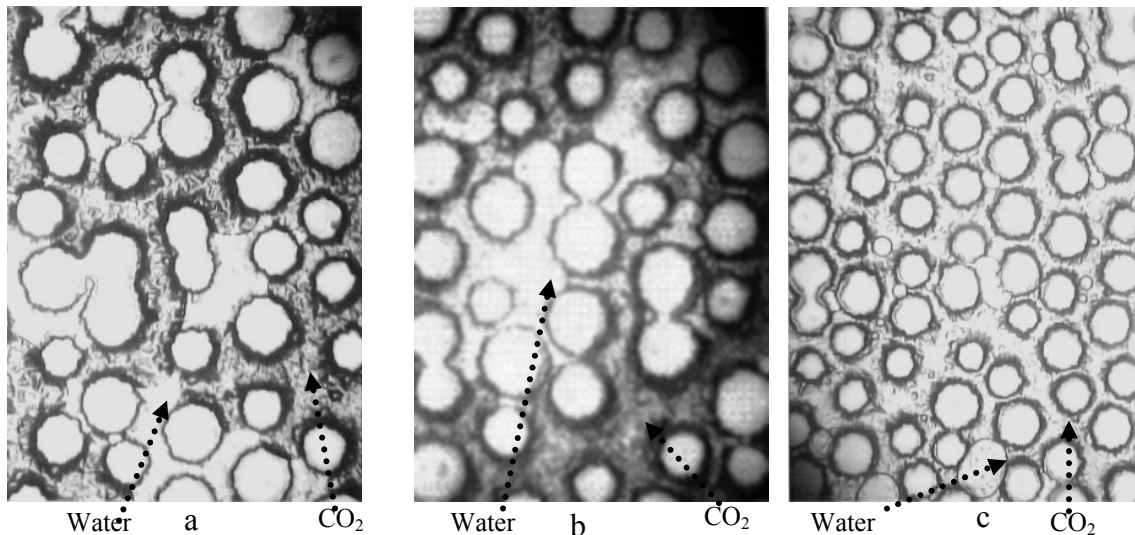


Figure 5: Intermediate-wet micromodel: (a) gaseous  $\text{CO}_2$  (60 bar,  $25^\circ\text{C}$ ) – (b) supercritical  $\text{CO}_2$  (100 bar,  $60^\circ\text{C}$ ) – (c) liquid  $\text{CO}_2$  (100bar,  $25^\circ\text{C}$ )

The experiments at higher pressures (Fig. 4b, 4c, 5b and 5c) show a different phase distribution. In some regions the water can be observed as a dispersed phase. Additionally, the shape of the interfaces shows that in this case the CO<sub>2</sub> behaves as the wetting phase. In these figures it can be observed that the wettability of the CO<sub>2</sub> is stronger at low temperatures. This could be probably related to a higher dissolution of CO<sub>2</sub> into water (lower pH) which reduces the electrostatic forces that tended to stabilize the water films.

## **INTERPRETATION USING A PORE NETWORK MODEL AND RESERVOIR SIMULATION**

The objective of this section is to use the pore network approach in order to quantify the effect of a possible CO<sub>2</sub> wetting behavior on capillary pressure curves, and then to use a numerical reservoir simulator to evaluate the impact of these new Pc curves at the Darcy scale, in a core sample and in an infinite saline aquifer. Detailed description of the pore network model (PNM) in terms of approach, model characteristics and construction can be found elsewhere (Laroche and Vizika, 2005). The network consists of a three-dimensional cubic lattice, formed by pore-bodies (nodes) interconnected by pore-throats (bonds), respecting the converging-diverging nature of the pores. The initial parameterization is based on experimental measurements characterizing the rock structure (mercury porosimetry) and also the macroscopic petrophysical properties (porosity, permeability). This approach was applied to Sample 1, a carbonate core sample used in a previous CO<sub>2</sub> flooding study (Egermann et al., 2006b). Figure 6a shows a very good agreement between the experimental capillary pressure and the best match of the PNM. More details about the use of this PNM can be founded elsewhere (Egermann et al., 2005). Figure 6b also shows a very good agreement between the gas/water relative permeability curves calculated by simulating gas invasion in a network fully saturated with water and those obtained experimentally, using a standard Unsteady State technique interpreted with full account of capillary end effects. For this calculation we used a contact angle of 0°, because of the strong water wettability of the sample.

In order to evaluate the effect of a partial wettability to CO<sub>2</sub>, a set of simulations using different contact angles (0°, 50°, 80°) was ran with PNM. Figure 7 shows the Pc curve obtained for each contact angle. It can be seen that there is an important water trap once the water wettability is reduced (higher contact angles). This is the consequence of a lower connectivity of the water phase that can be explained by the partial wettability to CO<sub>2</sub>.

### **The Core Scale**

The Pc and kr curves were introduced as input data in a numerical reservoir simulation model which was previously parameterized to the history matching of several CO<sub>2</sub> flooding experiments performed on a carbonate core. The parameters of the modeling at the core scale are presented in Table 1. The results for each contact angle in terms of brine production, pressure drop and CO<sub>2</sub> breakthrough are shown in Figure 8.

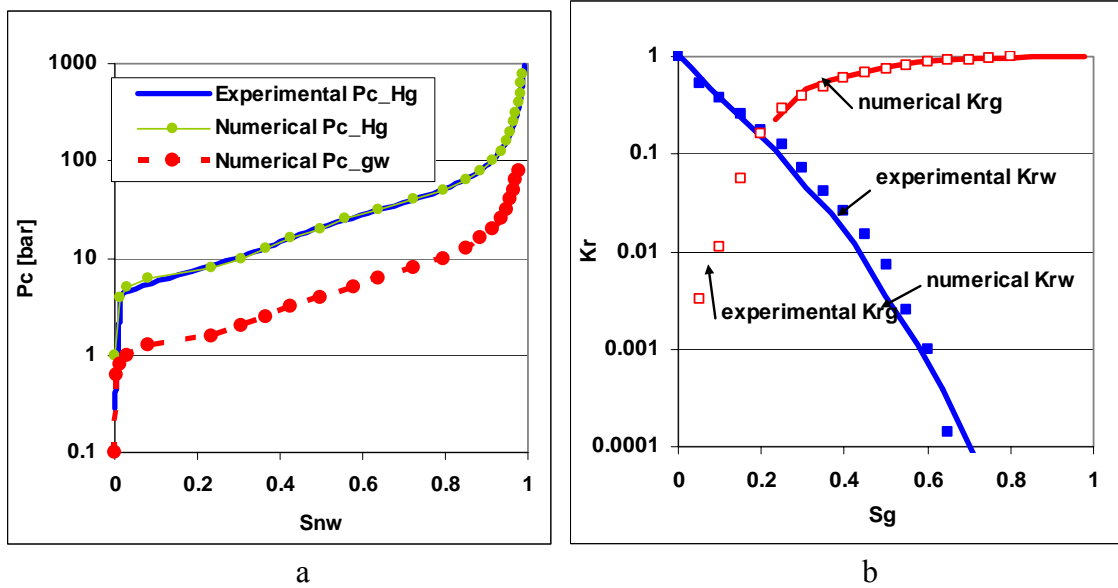


Figure 6: (a) Comparison between experimental and numerical mercury Pc curves and gas/water Pc curve scaled from Pc<sub>Hg</sub>. - (b) Comparison between experimental and numerical gas/water kr curves. (Egermann et al., 2005)

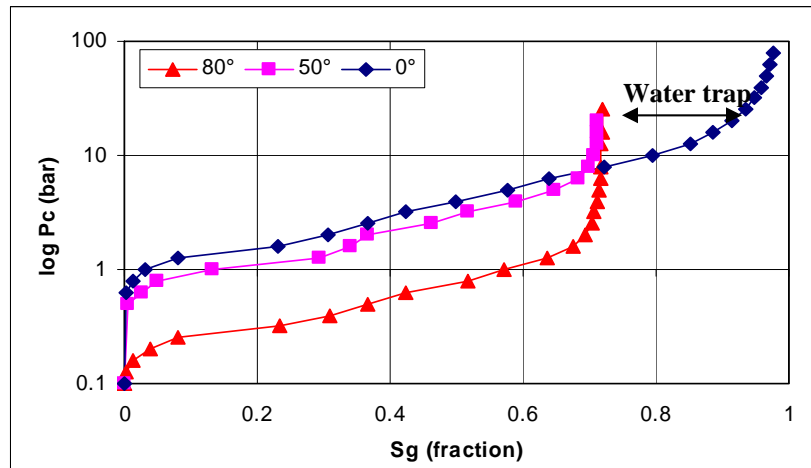


Figure 7: Pc curves from PNM for different contact angles.

Table 1. Simulation model at the core scale

K <sub>abs</sub> (mD)	φ (%)	L (cm)	D (cm)	PV (cm <sup>3</sup> )	Grid XYZ	P (bar)	T (°C)	Salinity (g/L NaCl)	Q <sub>CO2</sub> (cm <sup>3</sup> /h)
2.0	23	20	4.93	84.99	100x1x1	100	80	5.0	5.0



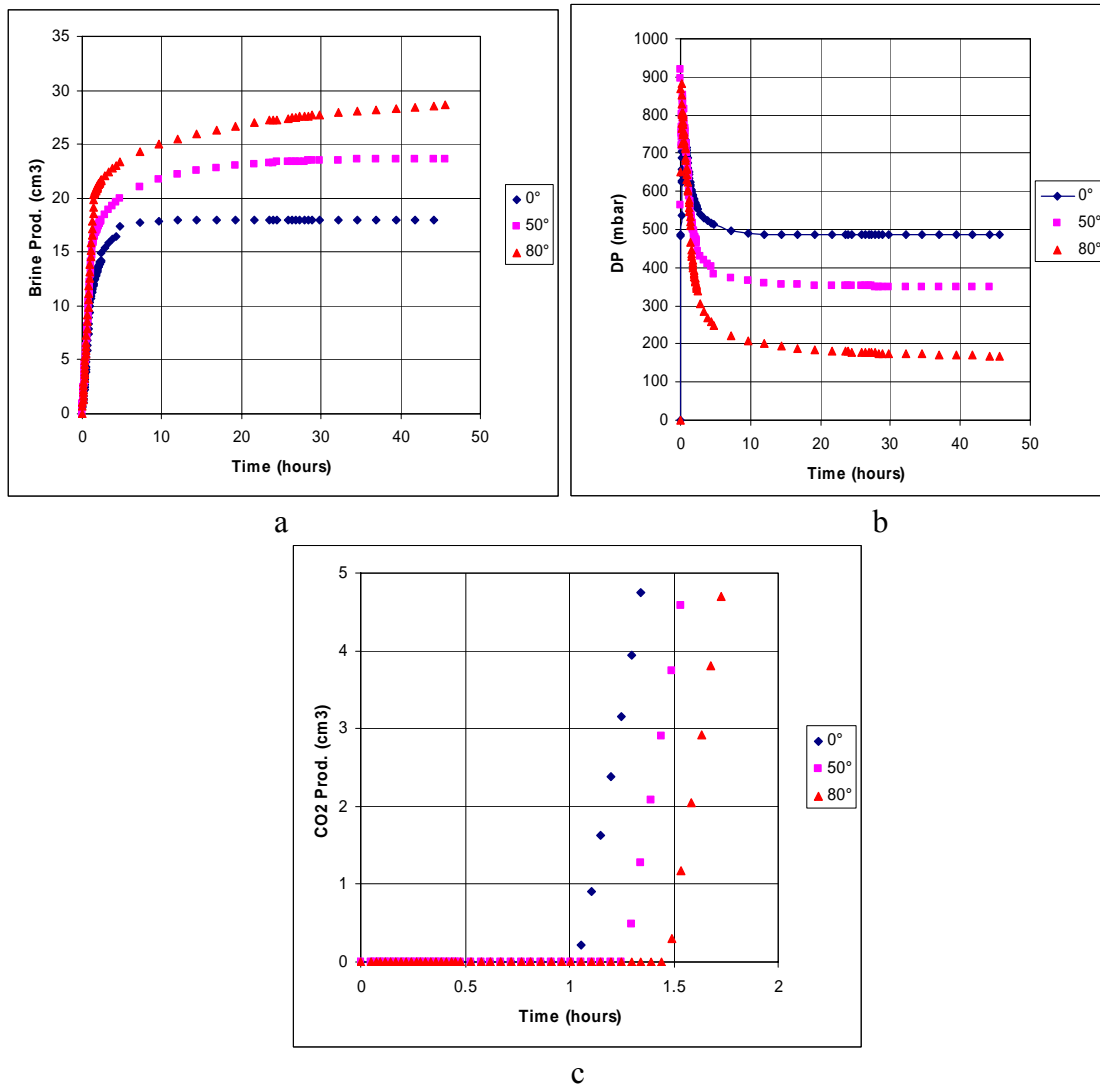


Figure 8: Results of the reservoir simulation at the core scale (a) Brine production. - (b) Pressure drop or differential pressure. - (c) CO<sub>2</sub> Breakthrough

Fig. 8a shows an increase in brine production while increasing the contact angle (or the affinity solid surface-CO<sub>2</sub>). This means that the water displacement process from a CO<sub>2</sub> injection is going to be considerably more efficient if the CO<sub>2</sub> wets, at least partially, the rock. We also observe in the same figure that the brine production plateau needs more time to be reached once the CO<sub>2</sub> partially wets the solid. This is consistent with Fig. 8c which shows a later CO<sub>2</sub> breakthrough while increasing the contact angle. At the pore scale, an increase in the CO<sub>2</sub>/substrate affinity would allow the CO<sub>2</sub> to flow in smaller pores which were not accessible in the case of a strongly water-wet system. Fig. 8b shows the evolution of the differential pressure (DP) while increasing the contact angle. After the CO<sub>2</sub> breakthrough the brine flow is very small, hence the DP is given by the amount of water that has been removed from the core. As the higher contact angle enables to reach a better sweep efficiency, the corresponding stabilized DP is smaller. This denotes a better injectivity index.

## The Reservoir Scale

In order to study the wettability influence at the reservoir scale, we simulated the CO<sub>2</sub> injection in a homogeneous infinite aquifer. For this we looked for representative conditions in terms of absolute permeability, amount of CO<sub>2</sub> injected, aquifer size, etc. As we mentioned before we limited our investigation to the effect of wettability on Pc curves. The parameters of this simulation model at the reservoir scale are shown in Table 2. We chose a radial mesh in order to investigate the near-wellbore region. CO<sub>2</sub> was injected by the bottom of the aquifers, at 95 m and 85 m from the top.

Table 2. Simulation model at the reservoir scale

K <sub>abs</sub> (D)	φ (%)	Rmax. (m)	Rmin. (m)	Thick (m)	Grid RTZ	P (bar)	T (°C)	Salinity. (g/L NaCl)	Q <sub>CO2</sub> (cm <sup>3</sup> /day)
1.0 – 0.2	23	10000	0.178	100	200x1x10	100	80	5.0	1e+06

We have introduced the Pc curves shown in Fig. 7, after modification according to the Leverett function for the new K<sub>abs</sub>. At this scale, we focused on two factors: injectivity and CO<sub>2</sub> distribution. Fig. 9 shows the injection pressure versus time for 1 D and 0.2 D.

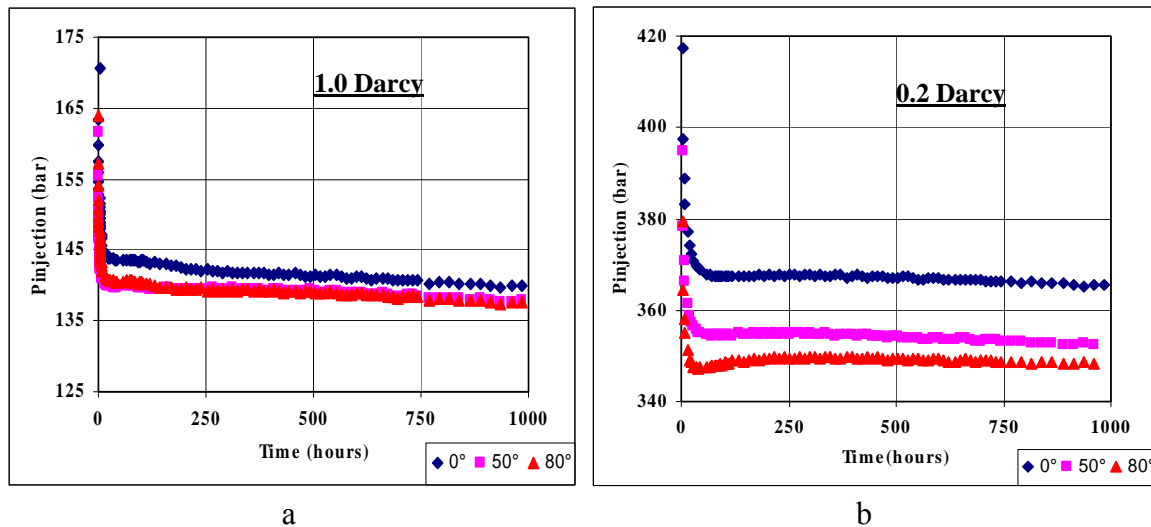


Figure 9: CO<sub>2</sub> injection pressure (a) 1.0 Darcy. - (b) 0.2 Darcy.

From Fig. 9, we observe that for a K<sub>abs</sub> of 1 D, the injection pressure after 40 days (960 hours) of injection does not depend very much on contact angles. For a K<sub>abs</sub> of 0.2 D, this difference becomes more significant, so the wettability seems then to have a significant effect on the injectivity. However, the over pressure in the reservoir (injection pressure - initial reservoir pressure) is also very high compared to that corresponding to a permeability of 1 D (270 bar vs. 40 bar). Even if the differences of injection pressure related to the wettability conditions seem very low compared to the global over pressure, at this CO<sub>2</sub> flow rate, each 1 bar of injecting pressure correspond to 75 t/d of CO<sub>2</sub>.

Concerning the distribution of the CO<sub>2</sub> in the aquifer, we focused on the radial penetration of the CO<sub>2</sub>. Due to the density difference between CO<sub>2</sub> and brine, CO<sub>2</sub> migrates to the top of the aquifer, so even if it is injected at the bottom of the formation, it is going to reach a longer distance at the top of the reservoir in a relatively short period.

We use this radial model to estimate the radial penetration (maximal spatial extent) of the injected CO<sub>2</sub> at different wettability conditions. This is particularly important if there are a significant number of wells that can be contacted by the CO<sub>2</sub> plume. Each of these wells provides a preferential flow path through which CO<sub>2</sub> can escape. If we compare a contact angle of 0° (strongly water-wet) vs. a contact angle of 80° (intermediate-wet) we obtained for the first a maximal spatial extent of 1400 meters and for the second 1600 m. The difference between both values is related to the water trap shown in Fig. 7. Nordbotten *et al.* (2005) proposed an analytical solution to estimate the maximal spatial extent of the injected CO<sub>2</sub> in a water-wet deep saline aquifer. This solution is based on energy minimization and reduces to a simple radial form of the Buckley-Leverett solution for conditions of viscous domination. It has already been compared to numerical reservoir simulation for a wide range of CO<sub>2</sub> injection scenarios. In order to compare our simulation model results to this equation, we modified our model in order to inject the same flow rate through all the vertical grids. We kept the overall conditions of Table 2 and a contact angle of 0°. We obtained a maximal spatial extent of 1323 m compared to 1498 m with the analytical solution. Part of this difference can be explained by the size of the grids far from the wellbore. Simulations conducted with the radial geometry also confirm that the injectivity index is improved when contact angle increases. By reference to the 0.2 D case, a 7% increase of injectivity can be expected with a modified contact angle.

## CONCLUSIONS

Based on micromodel experiments, we established that for water/CO<sub>2</sub> system, the CO<sub>2</sub> can wet the surface at reservoir conditions, if the solid surface is intermediate-wet or oil-wet. A Pore Network Model approach was used to explore the effects of a CO<sub>2</sub> partial wettability at the core scale and at the reservoir scale, for thermodynamic and operating conditions similar to those of CO<sub>2</sub> storage. The use of this approach allowed upscaling our observations from the pore scale to the Darcy scale by means of the capillary pressure. We observed that, at the core scale, the pressure drop along the sample is strongly affected by a change in the wetting conditions. At the core scale, the capillary pressure is the main factor in the pressure drop but at the reservoir scale it has a very low impact compared to viscous forces. At the reservoir scale, we showed that different wettability scenarios lead to different spatial extents of the injected CO<sub>2</sub> and injectivity index.

In terms of the reservoir integrity, a wetting behavior of the CO<sub>2</sub> could lead to an earlier capillary breakthrough through the caprock (see equation 1). According to Chiquet (2004), the effect of the diffusion of CO<sub>2</sub> into the caprock brine is very limited compared a capillary breakthrough, in terms of CO<sub>2</sub> leakage.

## ACKNOWLEDGMENTS

The authors want to thank IFP for permission to publish these results and S. Shaïek for her contribution in the experimental work.

## NOMENCLATURE

$K_{abs}$	Absolute permeability
$P_c$	Capillary pressure
$P_{brine}$	Pressure of the brine-rich phase
$P_{CO_2}$	Pressure of the CO <sub>2</sub> -rich phase
$P_c^{th}$	Capillary pressure breakthrough
$R_{throat}^{max}$	Largest connected pore throats or microfractures in the caprock
$R_{min}$	Minimum grid radius in the reservoir simulation model
$R_{max}$	Maximum grid radius in the reservoir simulation model
RTZ	Radial co-ordinates. R, radial axis; T, angular width of cells; Z, z axis.
$\theta$	Contact angle in the wetting phase
$\gamma$	Interfacial Tension

## REFERENCES

- Chiquet, P., Broseta, D. and Thibeau, S.: "Capillary Alteration of Shaly Caprocks by Carbon Dioxide", paper SPE 94183, presented at the 2004 Europec Biennial Conference, Madrid, June 13-16.
- Craig, F.F., "The Reservoir Engineering Aspects of Waterflooding", Monograph Series, SPE, (1971), Richardson, Texas, **3**.
- Derjaguin, B.V. and Landau, L., *Acta Physicochim URSS*, (1941), **14**, 633-662.
- Egermann, P., Lombard, J-M. and Bretonnier, P.: "A Fast and Accurate Method to Measure Threshold Capillary Pressures Under Representative Conditions", paper SCA A46, presented at the 2006a SCA International Symposium, Trondheim, Sept. 18-22.
- Egermann, P., Chalbaud, C., Duquerroix, J-P. and Le Gallo, Y.: "An Integrated Approach to parameterize Reservoir Models for CO<sub>2</sub> Injection in Aquifers", paper SPE 102308, presented at the 2006b SPE ATCE, San Antonio, Sept. 24-27.
- Egermann, P. Békri, S., Vizika, O.: "An Integrated Approach to Assess the Petrophysical Properties of Rocks Altered by Rock/Fluid Interactions (CO<sub>2</sub> Injection)", paper SCA A3 presented at the 2005 SCA International Symposium, Toronto, Aug. 21-25.
- Laroche, C., and Vizika, O., "Two-Phase flow properties prediction from small-scale data using pore-network modeling", *Transport in Porous Media*, (2005), **61**, 1, 77.
- Nordbotten, J.M., Celia, M.A. and Bachu, S., "Injection and Storage of CO<sub>2</sub> in Deep Saline Aquifers: Analytical Solutions for CO<sub>2</sub> Plume Evolution During Injection", *Transport in Porous Media*, (2005), **58**, 339-360.
- Siemons, N., Buining, H., Castelijns, H. and Wolf, K-H.: "Pressure Dependence of the Contact Angle in a CO<sub>2</sub>-H<sub>2</sub>O-Coal System", *Journal of Colloids and Interface Science*, (2006), **297**, 755-761.
- Thomas, K., Katz, D.L., Tek, M.R., "Threshold Pressure Phenomena in Porous Media", *SPE Journal*, (1968), June, 174.
- Verwey, E.J.W. and Overbeek, J.Th.G., *Theory of Stability of Lyophobic Colloids*, Ed. Elsevier, Amsterdam, (1948).
- "Overview of Long Term Framework for CO<sub>2</sub> Capture and Storage", IEA, (2004), Report number PH4/35, Nov.